

Supporting Information

Europium ions modulated room temperature phosphorescence in dye-encapsulated MOFs for dual-modal fluorescence-afterglow

Jiabo Chen^a, Renrui Sun^a, Wanjun Yang^a, Feifei Xing^a, Xiaolin Yu^b and Lining Sun^{a,*}

*Corresponding author

^a Department of Chemistry, College of Sciences, Shanghai University, Shanghai 200444, China. E-mail: lnsun@shu.edu.cn

^b Nikolaev Institute of Inorganic Chemistry, Siberian Branch of the Russian Academy of Sciences, 3 Lavrentiev Ave., 630090, Novosibirsk, Russia

Experimental section

Chemicals and materials

All the chemicals were used directly without further purification. $\text{LuCl}_3 \cdot 6\text{H}_2\text{O}$ (99.9%) and $\text{EuCl}_3 \cdot 6\text{H}_2\text{O}$ (99.9%) were purchased from Sigma-Aldrich Co. Ltd. Formamide (CH_3NO , 99.5%), 4,4'-bipyridine, and Ethanol ($\text{C}_2\text{H}_6\text{O}$, 99.7%) were purchased from Aladdin Co. Ltd. Deionized water was prepared in the laboratory and used throughout the experiment.

Statistical Analysis

Average lifetime (τ_{AVG}) calculation:

$$\tau_{\text{AVG}} = \frac{\text{Rel}_1\% \times \tau_1^2 + \text{Rel}_2\% \times \tau_2^2}{\text{Rel}_1\% \times \tau_1 + \text{Rel}_2\% \times \tau_2}$$

Characterization

Single crystal X-ray diffraction data were measured on a Bruker D8 VENTURE DUO PHOTON III system equipped with an Incoatec Ius 3.0 Microfocus sealed tube ($\text{Cu K}\alpha$, $\lambda = 1.54178 \text{ \AA}$) and a Helios MX Multilayer Optic monochromator. The crystal structure was solved and refined using the Olex 2 Software Package. The crystal structures have been deposited at the Cambridge Crystallographic Data Center (CCDC) and allocated the deposition numbers: Lu-MOFs: (CCDC: 2356792). The information is available free of charge from the Website (<http://www.ccdc.cam.ac.uk>).

Powder X-ray diffraction (PXRD) patterns were collected on an 18 KW D/MAX2200 V PC X-ray powder diffractometer. Measurements were taken at room temperature in the 2θ range of $5 - 90^\circ$ with a step of 0.02° (2θ) and counting time of 0.2 s/step. The emission spectra were recorded by Edinburgh FS-5 fluorescence spectrometer (using a suitable short-pass filter to exclude the second-order emission from the xenon arc lamp). The scan slit is 0.5. The repeat is 1 and the dwell time is 0.2 s. The lifetime measurements were performed with a microsecond pulsed Xenon lamp and a picosecond pulsed diode laser ($375 \pm 10 \text{ nm}$). Scanning electron microscope (SEM) images, energy dispersive X-ray spectroscopy (EDS) images, and element mapping images were collected on the Apollo 300. Fourier-transform infrared (FT-IR) spectra were recorded by an Avatar 370 instrument with a KBr pellet (spectral ranging from 4000 to 500 cm^{-1}). Yielded metal composition ratios were analyzed by inductively

coupled plasma atomic emission spectroscopy (ICP-AES) on PERKINE 7300DV. Optical diffuse reflection spectra were obtained at room temperature by Shimazu UV-3600i UV-visible spectrometer. The wavelength range of data acquisition is 200-1000 nm. Barium sulfate powder is used as the standard (100% reflectivity). Thermogravimetric analysis (TGA) experiments were carried out on NETZSCH STA449 F5 thermal analyzer from room temperature to 800 °C under a nitrogen atmosphere at a heating rate of 10 °C/min. All photos were taken with a digital camera (Nikon, D850).

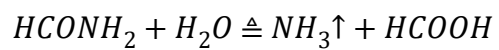


Fig. S1 Formamide gradually reacts with water to form ammonia and formic acid under heating.

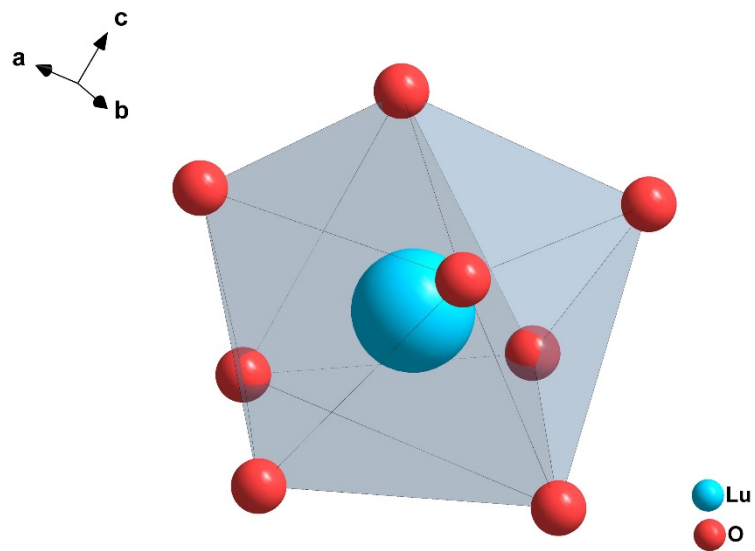


Fig. S2 Coordination polyhedron representation of Lu-MOFs.

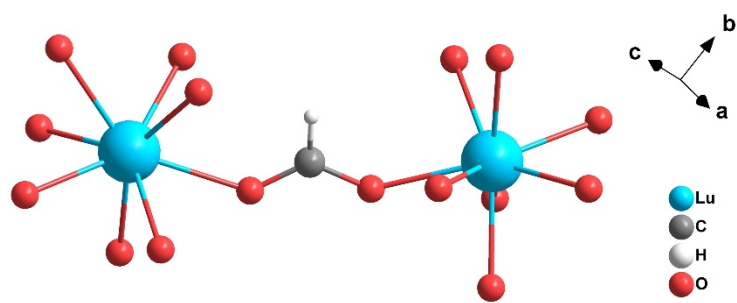


Fig. S3 The coordination environment and bridging fashion of formic acid ligand in Lu-MOFs.

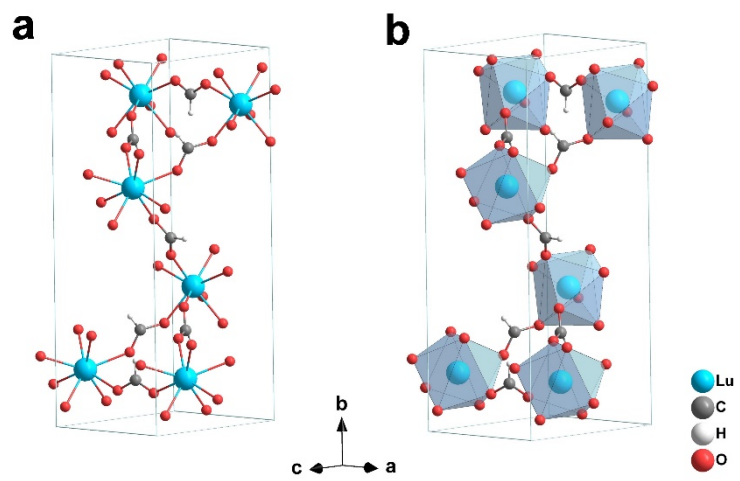


Fig. S4 A unit cell of Lu-MOFs.

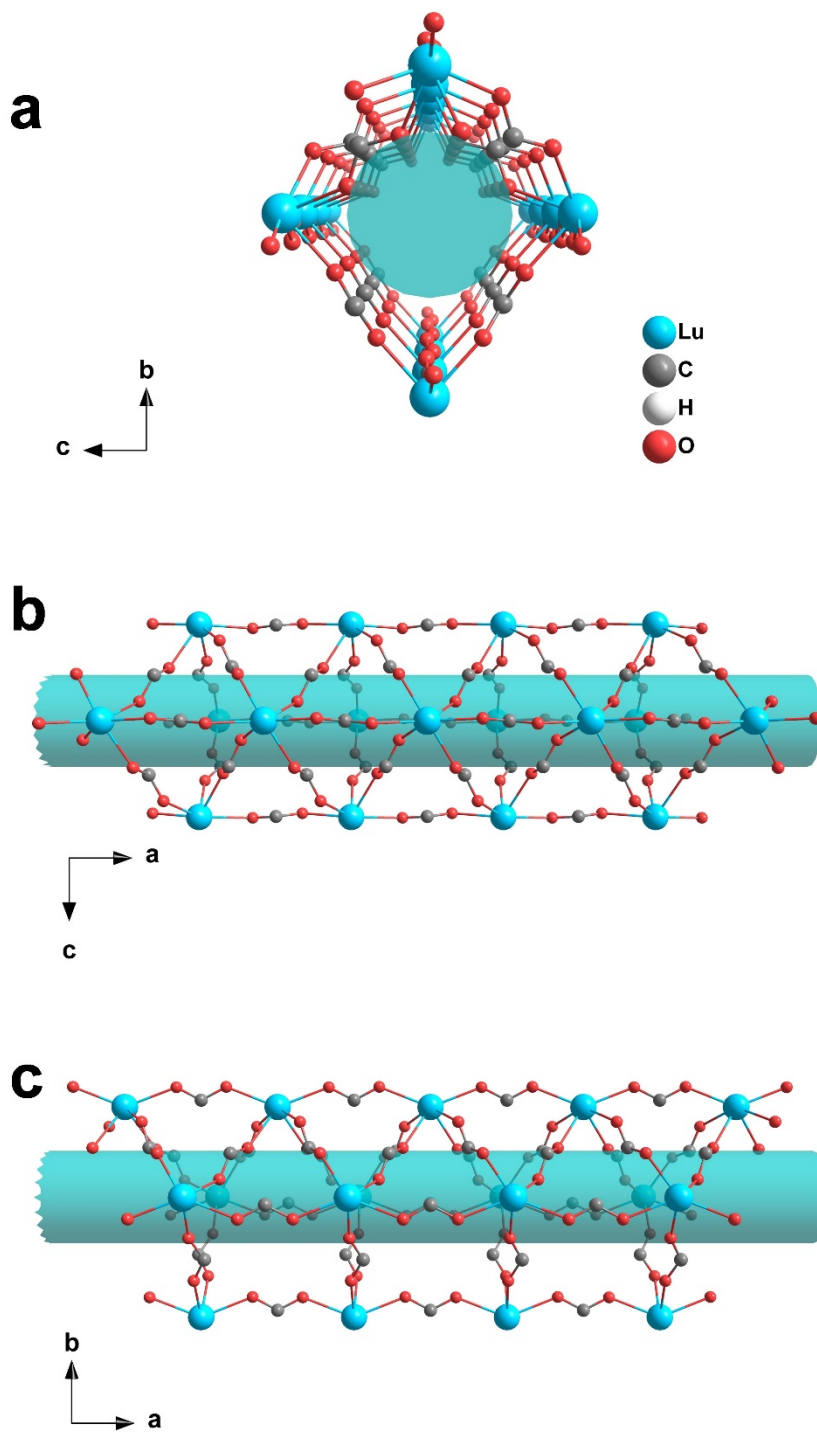


Fig. S5 Schematic representation of the structure of Lu-MOFs along the crystallographic axis a, b and c, respectively.

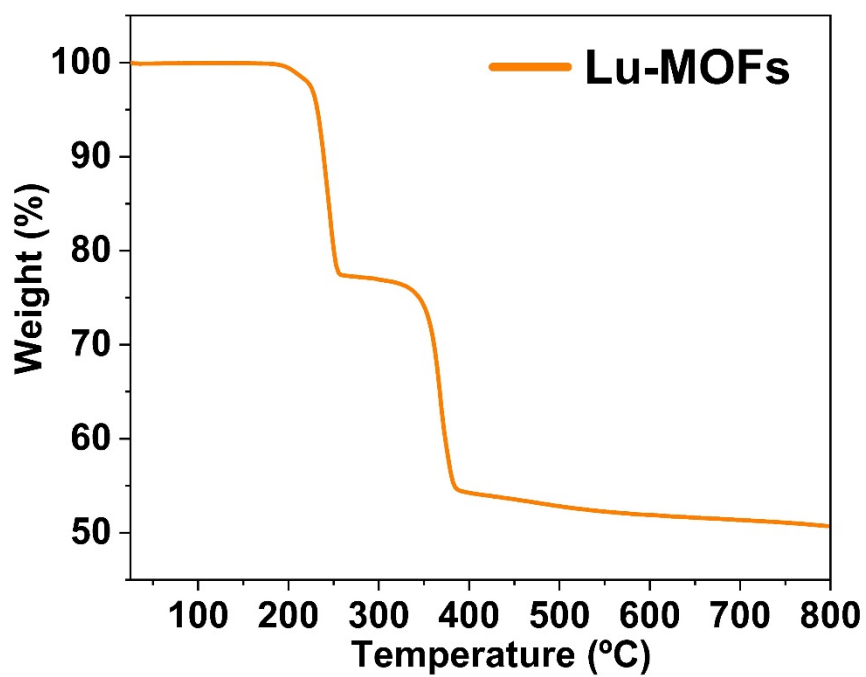


Fig. S6 Thermogravimetric analysis curve of Lu-MOFs.

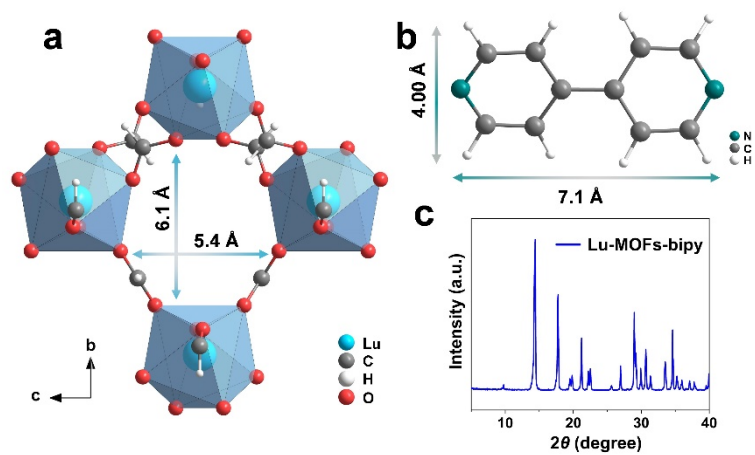


Fig. S7 (a) Pore size of Lu-MOFs. (b) The chemical structure and size of a 4,4'-bipyridine molecule. (c) Powder X-ray diffraction (PXRD) pattern of Lu-MOFs-bipy.

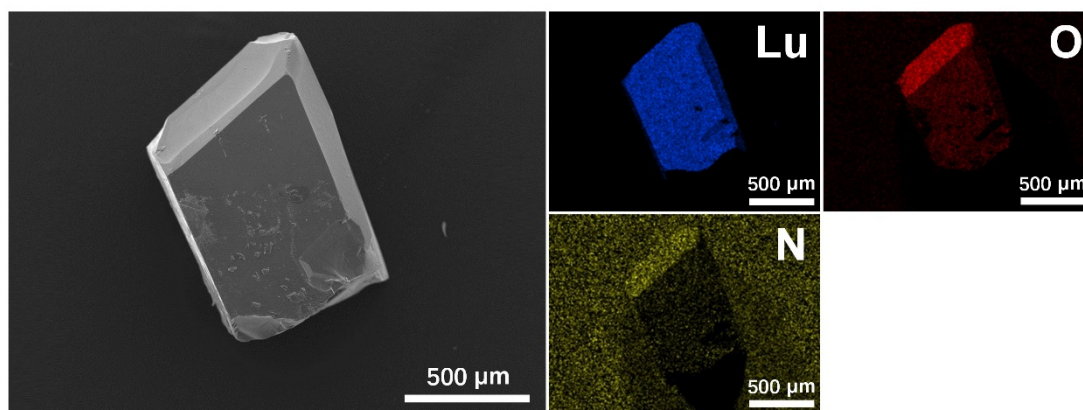


Fig. S8 Scanning electron microscopy (SEM) image of Lu-MOFs-bipy and energy dispersive X-ray spectroscopic (EDS) mappings of Lu, O, and N elements.

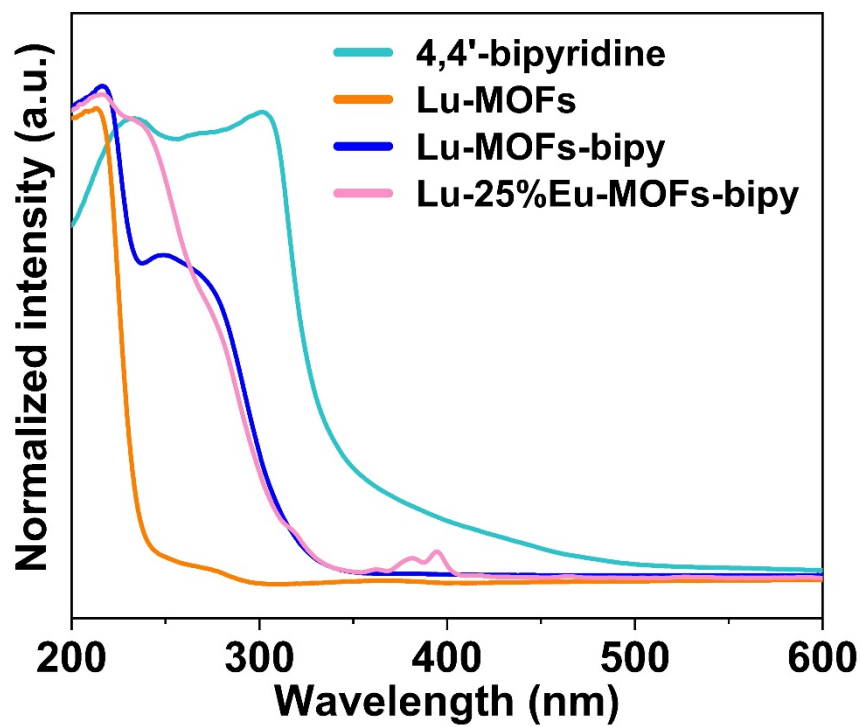


Fig. S9 UV-vis absorption spectra of 4,4'-bipyridine, Lu-MOFs, Lu-MOFs-bipy and Lu-25%Eu-MOFs-bipy in solid state.

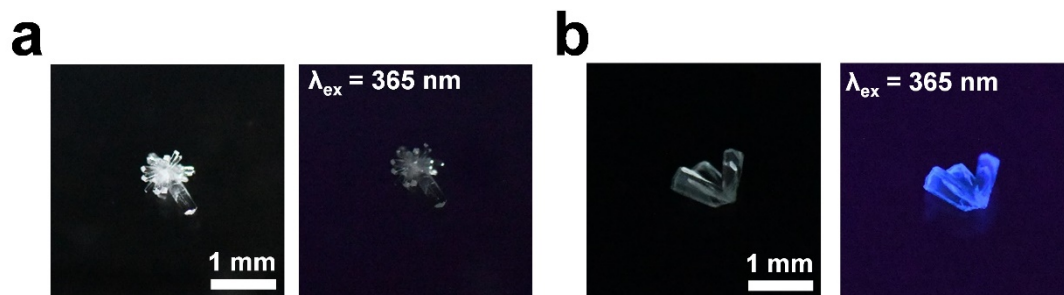


Fig. S10 Photographs of (a) Lu-MOFs crystal and (b) Lu-MOFs-bipy crystal under natural light and 365 nm excitation.

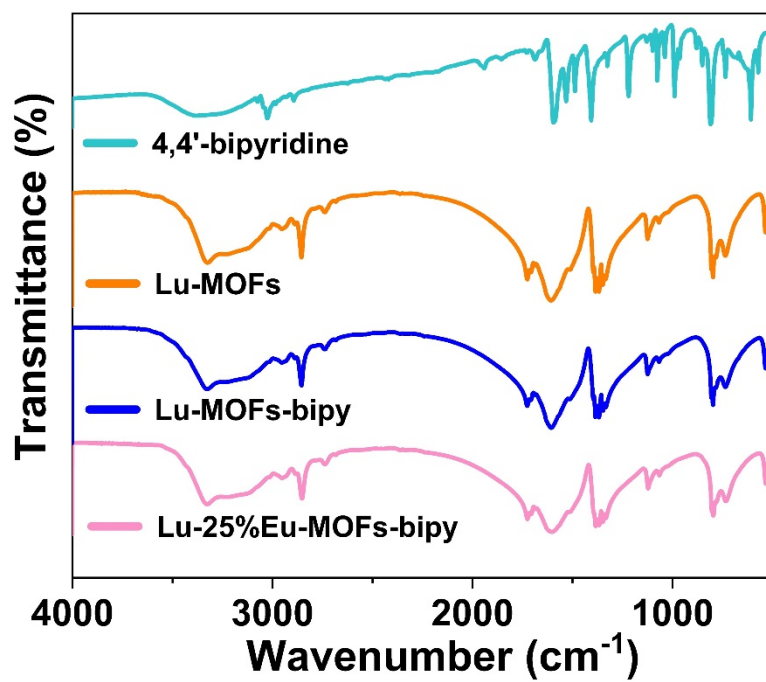


Fig. S11 Fourier-transform infrared (FT-IR) spectra of 4,4'-bipyridine, Lu-MOFs, Lu-MOFs-bipy, and Lu-25%Eu-MOFs-bipy.

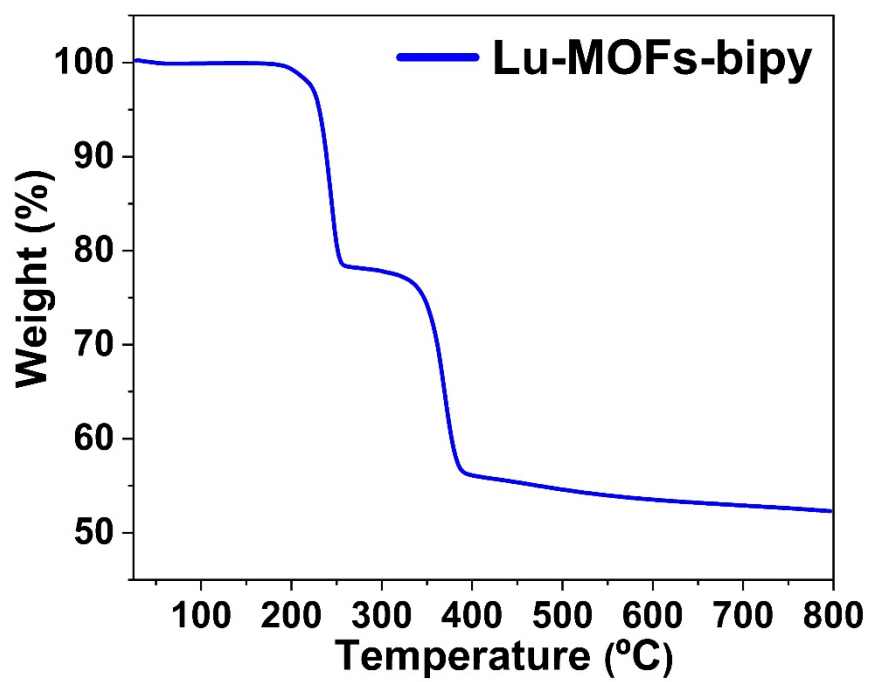


Fig. S12 Thermogravimetric analysis curve of Lu-MOFs-bipy.

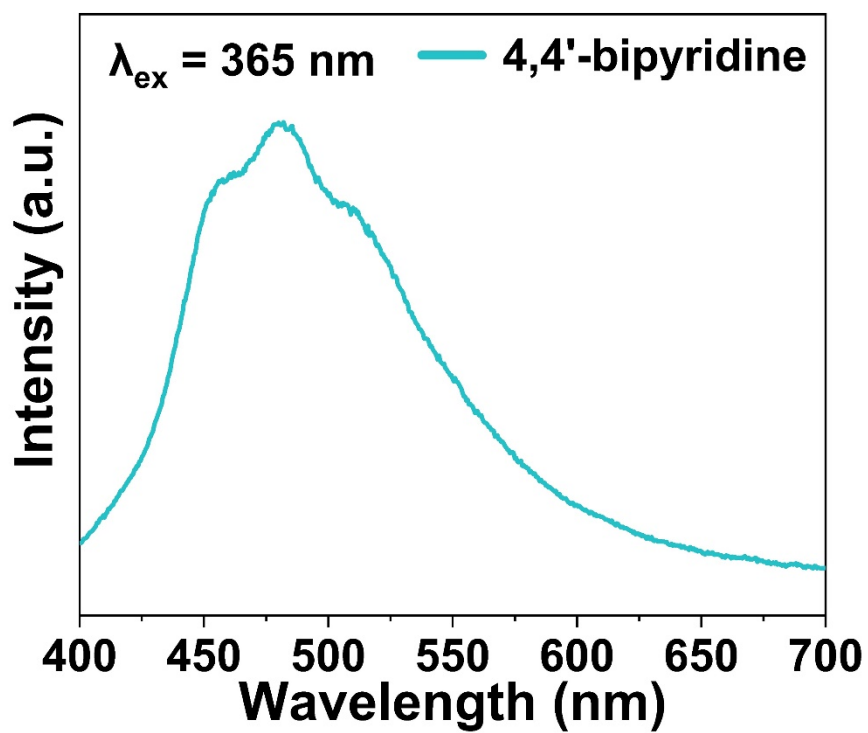


Fig. S13 The solid-state emission spectrum of 4,4'-bipyridine at room temperature under 365 nm excitation

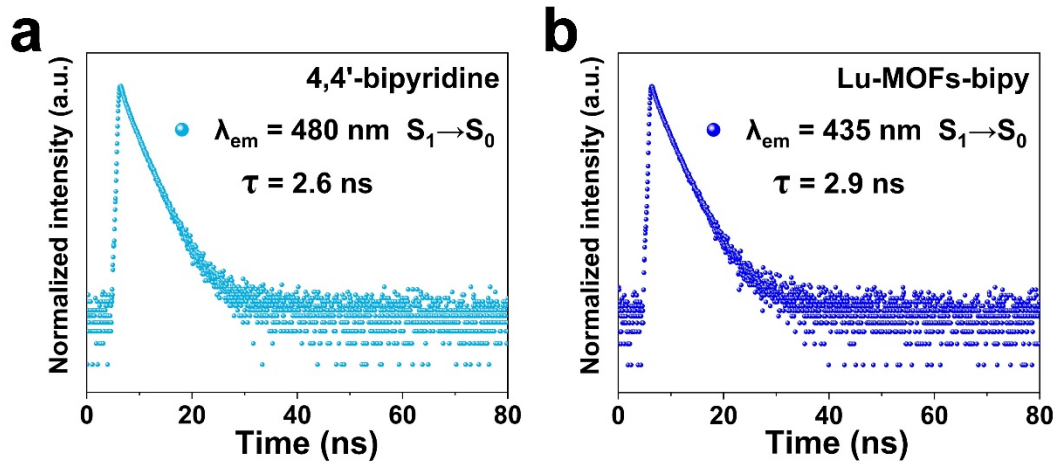


Fig. S14 Decay curves of emissions at 480 nm for 4,4'-bipyridine and at 435 nm for Lu-MOFs-bipy under pulsed excitation of 375 nm.

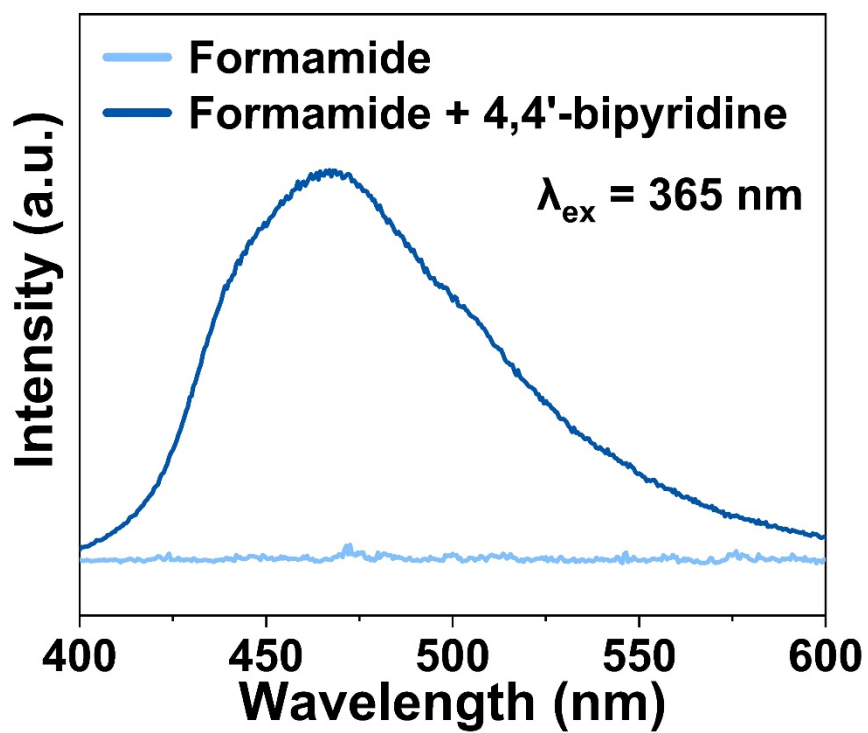


Fig. S15 The fluorescence spectra of formamide and 0.5 mmol 4,4'-bipyridine dissolved in 2 mL formamide.

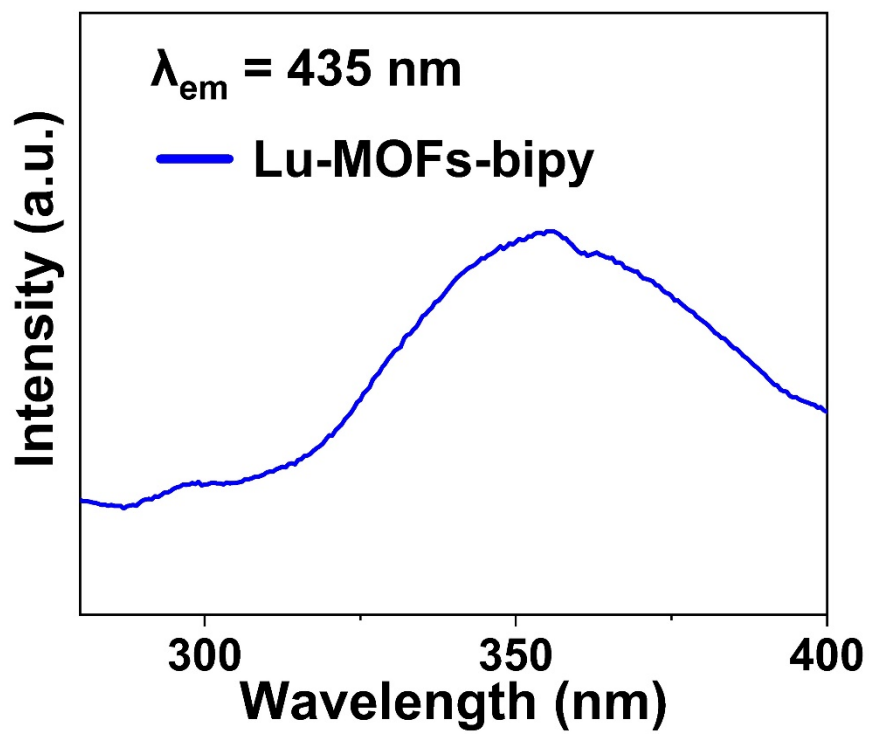


Fig. S16 Excitation spectrum of Lu-MOFs-bipy in solid state.

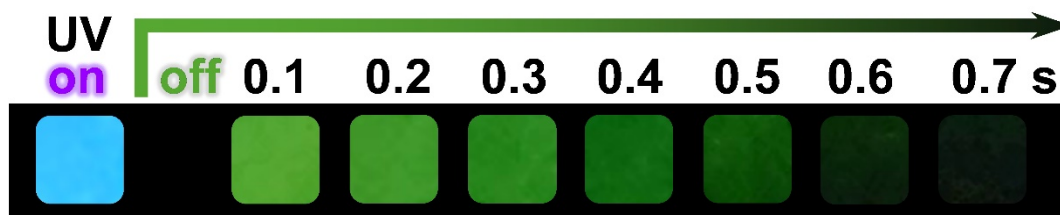


Fig. S17 Photographs of Lu-MOFs-bipy taken under 365 nm irradiation (UV on) and at different time intervals after removal of UV irradiation (UV off).

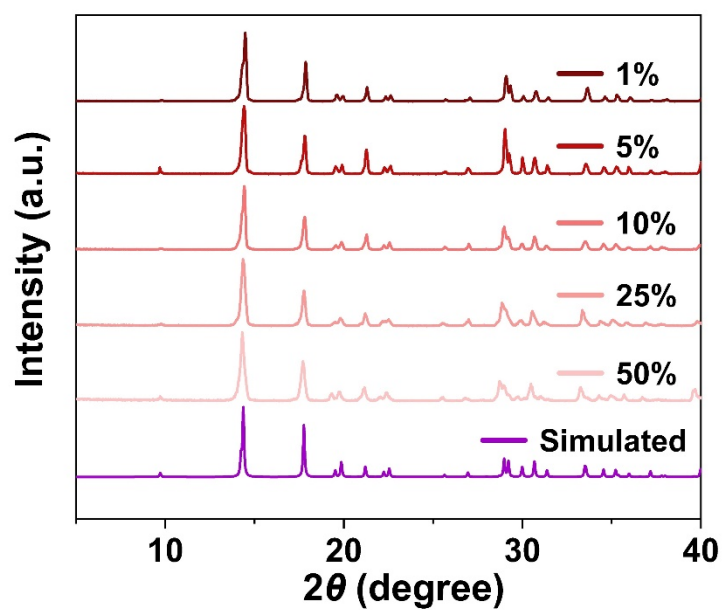


Fig. S18 PXRD patterns of Lu- x %Eu-MOFs-bipy ($x = 1, 5, 10, 25$ and 50), and simulated pattern of Lu-MOFs.

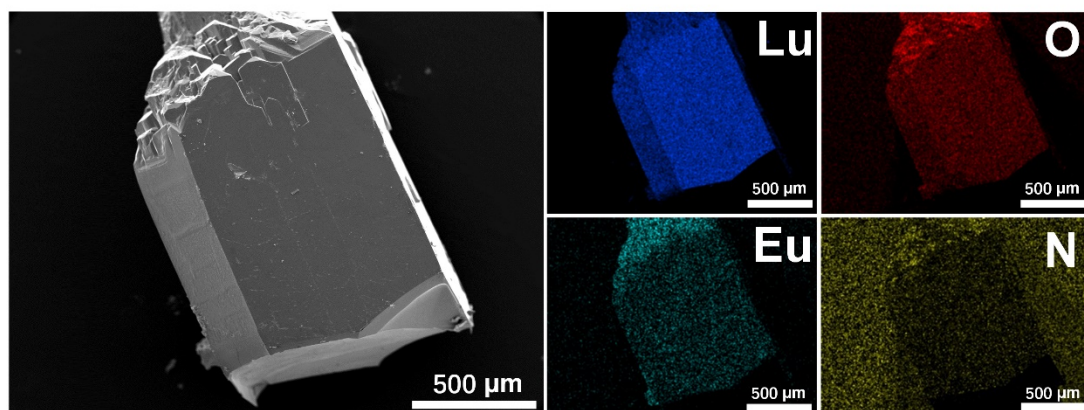


Fig. S19 SEM image of Lu-25%Eu-MOFs-bipy and EDS mappings of Lu, O, Eu, and N elements.

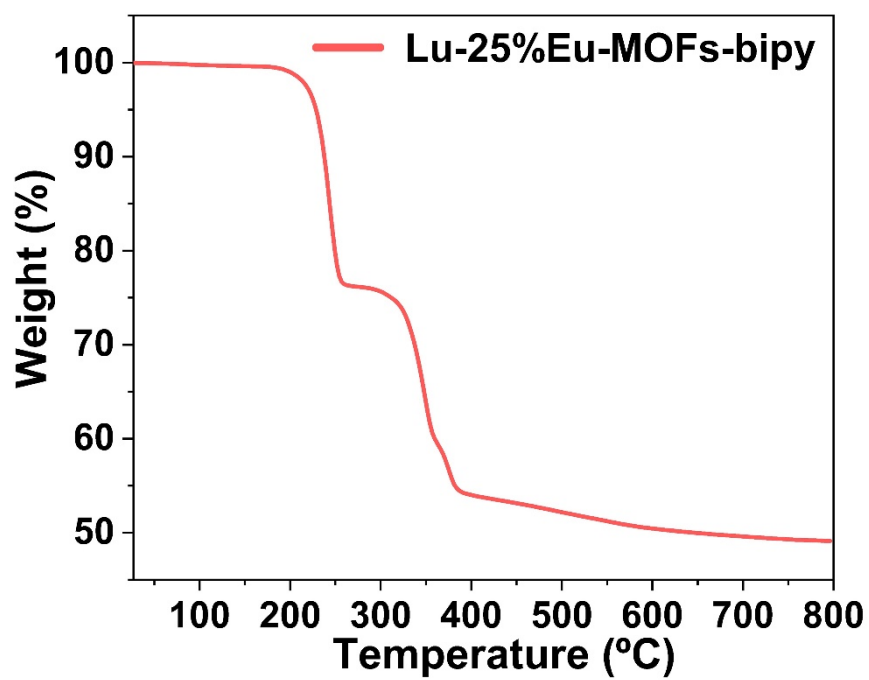


Fig. S20 Thermogravimetric analysis curve of Lu-25%Eu-MOFs-bipy.

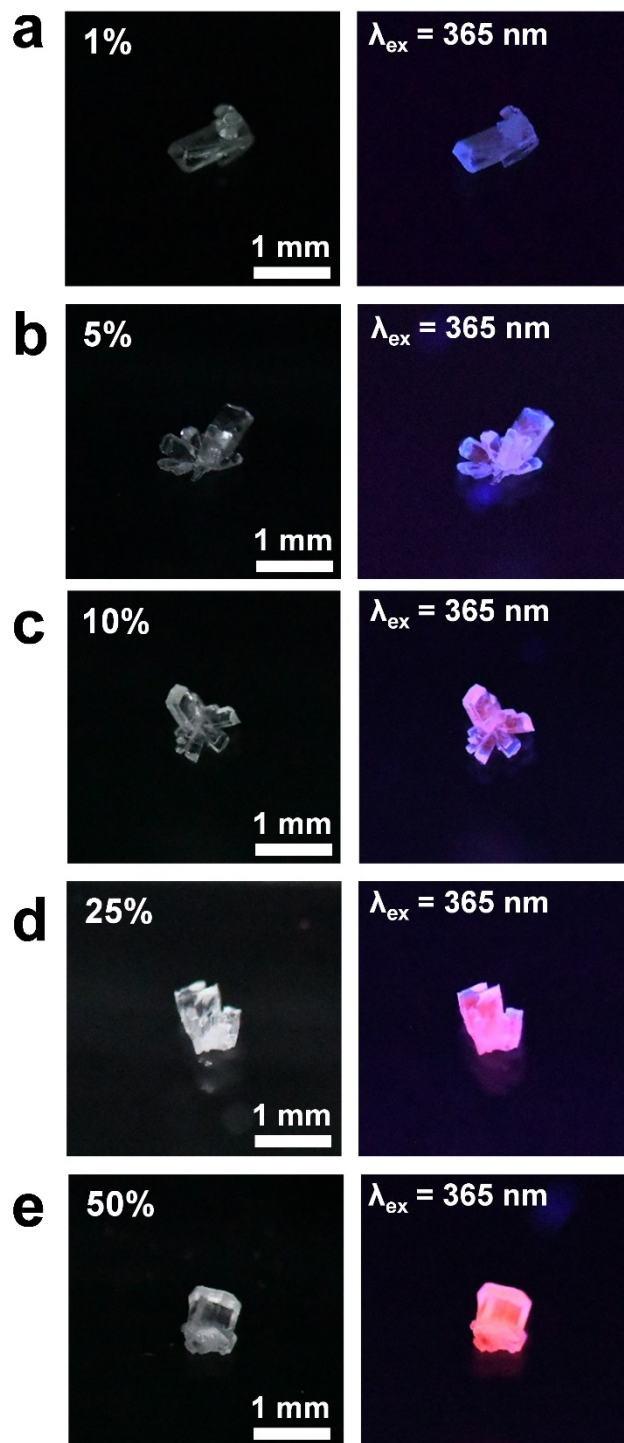


Fig. S21 Photographs of Lu- x %Eu-MOFs-bipy crystals under natural light and 365 nm excitation, respectively, taken with an optical camera. $x = 1$ (a), 5 (b), 10 (c), 25 (d), and 50 (e).

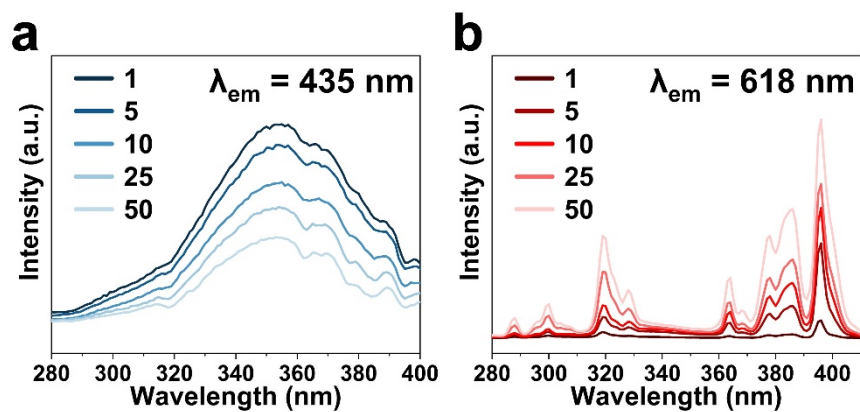


Fig. S22 Excitation spectra of Lu-*x*%Eu-MOFs-bipy (*x* = 1, 5, 10, 25, and 50) in the solid state monitored at 435 nm (a) and 618 nm (b), respectively.

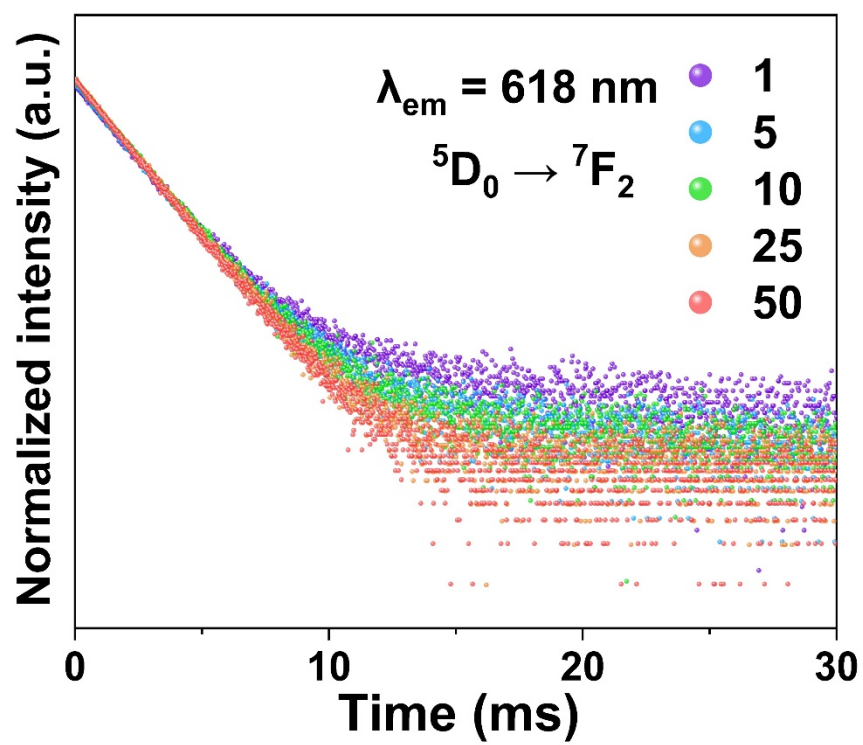


Fig. S23 Decay curves of the phosphorescence detected at 618 nm for Lu- x %Eu-MOFs-bipy ($x = 1, 5, 10, 25,$ and 50) under pulsed excitations of 365 nm.

Table S1. Crystal structure data for Lu-MOFs crystal.

Chemical Formula	C ₅ H ₅ O ₁₀ Lu
Temperature	300(2) K
Weight	400.06 g/mol
Crystal size	0.050x 0.050 x 0.100 mm
Crystal system	orthorhombic
Space group	C 2 2 2 ₁
Unit cell dimensions	a = 6.6112(3) Å b = 18.1762(9) Å c = 8.3723(4) Å α = 90° β = 90° γ = 90°
Unit cell volume	1006.07(8)
Z	4
Density (calculated)	2.641 g cm ⁻³

Table S2. Lu and Eu elements analyses of Lu- x %Eu-MOFs-bipy ($x = 1, 5, 10, 25,$ and 50) by inductively coupled plasma atomic emission spectroscopy (ICP-AES).

Compound	Molar ratio (%)	
	Lu	Eu
Lu-1%Eu-MOFs-bipy	98.91	1.09
Lu-5%Eu-MOFs-bipy	94.49	5.51
Lu-10%Eu-MOFs-bipy	89.05	10.95
Lu-25%Eu-MOFs-bipy	72.94	27.06
Lu-50%Eu-MOFs-bipy	51.52	48.48

Table S3. Fitting parameters for single exponential decay of Lu-*x*%Eu-MOFs-bipy (*x* = 1, 5, 10, 25, and 50) emitting at 435 nm (4,4'-bipyridine), 545 nm (4,4'-bipyridine), and 618 nm (Eu³⁺) under a picosecond pulsed diode laser (375 ± 10 nm) and a microsecond pulsed Xenon lamp (365 nm) excitation, respectively.

Eu³⁺ content	λ_{ex} = 375 nm	λ_{ex} = 365 nm	
	λ_{em} = 435 nm	λ_{em} = 545 nm	λ_{em} = 618 nm
1%	2.8 ns	108.0 ms	4.7 ms
5%	2.8 ns	101.8 ms	3.0 ms
10%	2.7 ns	99.2 ms	2.4 ms
25%	2.6 ns	88.4 ms	2.0 ms
50%	2.5 ns	86.8 ms	1.9 ms